2016

3D-CFD Design Study And Optimization Of A Centrifugal Turbo Compressor For The Operation In A Hybrid Sorption/ Compression Heat Pump Cycle

Thomas Eckert
University of Applied Sciences Munich, Germany, teckert@hm.edu

Leo Dostal
University of Applied Sciences Munich, Germany, leo.dostal@gmx.net

Martin Helm
University of Applied Sciences Munich, Germany, martin.helm@hm.edu

Christian Schweigler
University of Applied Sciences Munich, Germany, christian.schweigler@hm.edu

3D-CFD DESIGN STUDY AND OPTIMIZATION OF A CENTRIFUGAL TURBO COMPRESSOR FOR THE OPERATION IN A HYBRID SORPTION/COMPRESSION HEAT PUMP CYCLE

Thomas ECKERT*, Leo DOSTAL, Martin HELM, Christian SCHWEIGLER

Munich University of Applied Sciences,
Department 05: Building Services Engineering
Lothstraße 34, 80335 Munich, Germany
Email: teckert@hm.edu
Phone: +49 89 1265 4298

* Corresponding Author

ABSTRACT

In various applications the use of sorption chillers and heat pumps is limited by the available temperature level of the driving heat source or the heat sink for export of reject heat. These constraints can be overcome by integrating an efficient high-speed transonic turbo-compressor into the internal cycle of a thermally driven water/lithium bromide absorption heat pump. The operation in a hybrid heat pump with the refrigerant water implies specific challenges for the design of the compressor: Saturation pressures in the sub-atmospheric range, low vapor density, high volume flows and a targeted pressure ratio of 3 result in high impeller tip speed up to 660 m/s and transonic flow phenomena in the flow channel of impeller and diffusor. Here the authors present a theoretical design study based on a 3D-simulation of a centrifugal compressor, targeted at the given operating conditions for a hybrid heat pump. Key figures are investigated to figure out the relationship between impeller tip speed, compressor pressure ratio and operating range of the compressor meeting the requirements, wide stable operating range between surge and choke line and appropriate pressure ratio. The optimization of the impeller geometry comprises both fluid dynamic behavior and structural stability.

1. INTRODUCTION

In the field of building energy supply, the reduction of the electric power consumption for heating and cooling is a core issue. The dominating part of the electric demand is to be attributed to the operation of compression chillers serving for cooling and air-conditioning. As an alternative to mechanically driven devices, absorption chillers can be applied, activated by driving heat. Apart from directly fired multi-stage chillers (Ziegler *et al*, 1993), single-stage chillers driven by hot water from a district heating network or supplied by a cogeneration system or a solar thermal installation are available. A major obstacle for the use of these thermally driven chillers is their limited ability for the use of low-grade heat (Schweigler, 1999). For typical operating conditions in building air-conditioning systems the driving hot water can only be cooled down to about 80 °C.
This limitation can be overcome, if a mechanical vapor compressor is integrated into the sorption refrigeration cycle: At the expense of input of mechanical work, additional freedom for the design of the thermal cycle is gained (Alefeld and Ziegler, 1985), (Niebergall, 2011), (Ziegler, 1991) and (Ziegler, 2009). Either the temperature level of the driving heat source can be lowered, or the heat rejection of the chiller can operate at a higher temperature level, allowing for the use of dry cooling towers instead of wet open systems. A third option is to boost the cooling output in order to provide extra capacity during peak demand of the building (Eckert *et al*, 2015) and (Helm *et al*, 2015). Consequently, the application of sorption chillers in conjunction with low-grade heat sources and particularly in small scale systems is facilitated.

There have been some successful applications of vapor compressors using water as refrigerant (Koren and Ophir, 1996), (Madsboell, 2011), (Madsboell *et al*, 2015), (Madsboell and Minds, 1995) and (Paul, 2007). This publication focuses on the design of a small scale radial turbo compressor for the refrigerant water for a hybrid sorption/ compression heat pump system with an evaporator capacity of about 10 kW. The investigation is performed by coupled modeling of the fluid dynamic behavior and the structural-mechanic stability. The focus of this paper is the impeller aerodynamic design and the influence of key design parameters on the shape and the width of the operating envelope of the compressor under varying operating conditions. The characteristic target diagram for the compressor, based on an analysis of the operational envelope of the hybrid cycle heat pump, is being discussed in (Eckert *et al*, 2016).

2. USE OF WATER AS REFRIGERANT IN A HYBRID HEAT PUMP

2.1 Water Vapor Compressor

Comparing water (R718) to other refrigerants, e.g. R134a, it is characterized by a low molecular mass γ, a high sonic velocity c and a high isentropic coefficient κ. The cycle operates at sub-ambient pressures and its p-T curves lie under all common refrigerants (Mueller and Kharazi, 2006) at very low pressures. Thus the specific volumetric cooling capacity of water vapor is very low and therefore the volumetric flowrate for a desired specific cooling capacity and temperature lift can be up to a 100 times higher than the volumetric flowrate of a conventional refrigerant like R134a. Under the same conditions the required pressure ratio is nearly twice as high as for R134a. For a target pressure ratio of 3 a high circumferential Mach Number and isentropic work are required, which lead to a high impeller tip speed of up to 660 m/s, nearly four times higher than for R134a (Eckert *et al*, 2016). The temperature lift for a one-stage water vapor compressor is limited to roughly 20 K. A classical compression refrigeration system will require a two stage water vapor compressor. For a compression chiller using the water as refrigerant, the discharge temperature of the compressor is very high and has a negative influence of the energetic efficiency of the chiller. For water the irreversibility due to de-superheating of the compressed refrigerant vapor is substantially higher than for R134a (Mueller and Kharazi, 2006), but if the turbo compressor is used in a sorption/compression chiller, the superheat can be used for preheating the sorption sub-cycle of the hybrid chiller.

2.1 Hybrid Heat Pump System

To overcome the limitations of the single stage water vapor turbo compressor, a hybrid cycle concept can be applied for the refrigerant water. In this research the combination of a ”thermal compressor” with a mechanical compressor is investigated. The so called thermal compressor is a heat driven chiller and the combination of both systems is called hybrid chiller. A jet ejector working in the cycle could also be investigated (Sarevski and Sarevski, 2012), but the available pressure ratio is far below the minimum pressure ratio of 2 which is required for a sound design of the hybrid heat pump.

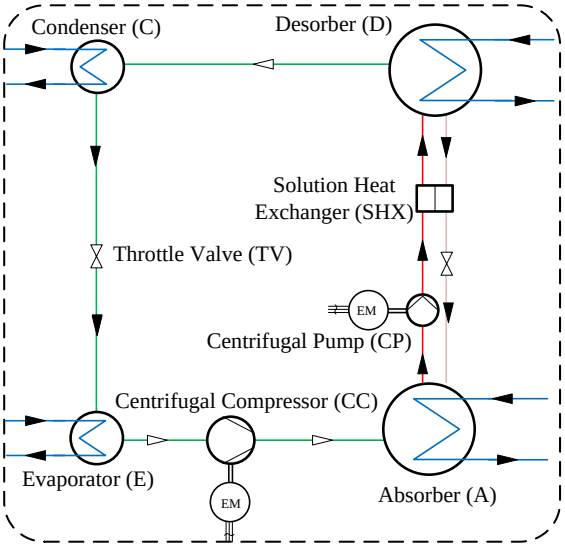

Figure 1: Schematic thermodynamic cycle of the hybrid heat pump in EVA mode

In figure 1 the schematic thermodynamic cycle of the hybrid heat pump in the EVA configuration with evaporator (E), condenser (C), centrifugal compressor (CC), solution heat exchanger (SHX), absorber (A) and desorber (D) is shown. In (Eckert *et al*, 2016) the target compressor map for the turbo compressor for different operating conditions is shown. This map lays out the compressor requirements for various cold water temperatures (6 °C to 15 °C), cold capacity (4 kW to 16 kW) and different settings of the electrical and heat factor EH (0.5 up to 1.5). This diagram is used to compare and evaluate the initial compressor designs.

3. MODELING TECHNIQUE AND BASIC DESIGN

3.1 Discretization and Boundary Conditions of Fluid Analysis

The computational meshes for the rotating and non-rotating fluid domains have been created by use of ANSYS-TurboGrid. An automated topology meshing system with high quality structural hexahedral mesh and local refinements was used. All domains, rotating and non-rotating, are designed as two separate structures and are connected at the interface between rotor and diffusor by usage of a frozen rotor interface. To reduce the computational effort, only one single passage of the flow field is being calculated. The heat transfer was calculated by the total energy heat transfer model. For the turbulence the SST model and for the heat transfer model Total Energy have been chosen. The calculation was carried out with the real gas IAPWS-IF97 water steam model. The use of the high resolution mode for the discretization of the Reynolds-averaged Navier-Stokes (RANS) equations boosted the accuracy in the results for the steady state solution.

The boundary conditions for the rotor are summarized in figure 2 and are set as follows: The flow condition at the impeller inlet was defined as a subsonic flow, by setting total temperature and total pressure input variables. The turbulence intensity in this section has been set to ”medium” with an intensity value of 5%. Periodic boundary conditions were defined to allow the reduced calculation of only one passage. The surfaces of hub and blade were defined as adiabatic walls with appropriate rotational velocities. The shroud was defined as a counter-rotating wall in order to reflect the motion of the rotor in relation to the fixed shroud. Because of the low ratio between tip clearance and blade width the return flow between impeller shroud and casing is ignored for the first optimization process. For the domain interfaces between inlet geometry and impeller and between impeller and diffusor ”Frozen Rotor” was chosen as domain interface type. This setting allowed for shorter computational time and higher accuracy, as compared to the ”Stage” interface mode. The impeller outlet cross section is matched with the diffusor inlet cross section and defined as ”Frozen Rotor”. The periodic limitations of the diffusor have been set as periodic boundaries. The hub and shroud surfaces were set as adiabatic wall boundaries. At the diffusor exit plane, the subsonic flow velocity was assured by limiting the mass flow rate (setup a). This setup is robust at the surge line, because the pressure ratio exhibits only a moderate increase with falling mass flow. At the choke line, operation of the compressor was characterized by total pressure at inlet and static pressure at outlet (setup b). This setup promises a more robust behavior at the choke line than setup a, where small changes of mass flow induce a strong decrease of the pressure ratio.

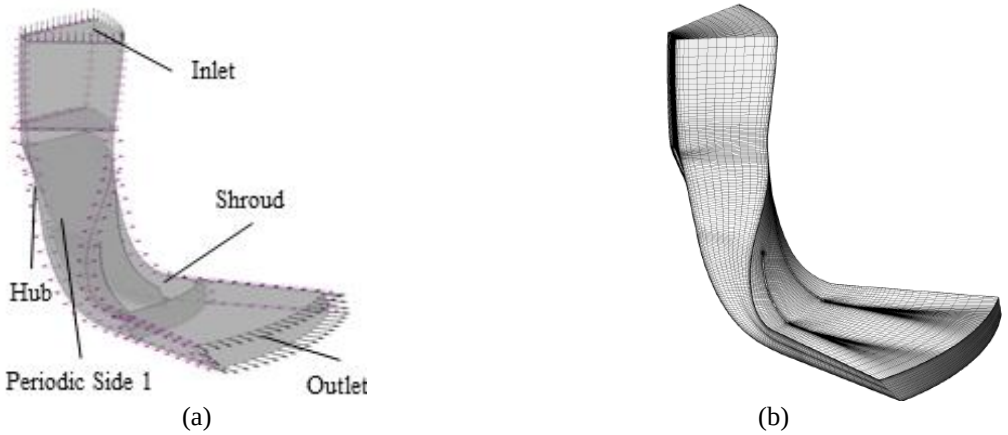

(a) (b)

Figure 2: Fluid flow blade passage with the boundary conditions (a) and structural meshing of the fluid flow passage (b)

3.2 Solver Settings

To achieve an adequate convergence the CFX solver settings had to be adjusted. As the optimal timescale is dependent on several influencing parameters, a fixed given physical timescale seemed unfeasible due to its relation to the rotational speed. Thus the conservative approach of auto timescale was chosen. To shift the simulation focus towards a faster convergence at the expense of stability, the auto timescale value was multiplied by an alterable factor, increasingly varying over the number of iterations. A factor value of 5 for up to 60 iterations followed by a factor of 20 turned out as a good trade-off between a fast and sufficiently robust convergence. To increase the speed of convergence the solver uses the current solver results as starting values, if possible. The calculation of characteristic diagrams therefore yields a so called mass flow ramp, resulting in increasing mass flow over iteration time to grant a higher robustness at the beginning of a simulation. Under consideration of the compressible medium and high stream velocities, the double precision calculation model was enabled to reach a more stable convergence towards the end of the calculation.

3.3 Structural Investigation

In the present modelling the ANSYS structural module is adopted providing a FEM procedure for determination of the von-Mises-stress distribution. The solid geometry for stress analysis is discretized by use of quadratic tetrahedral elements. In general, the centrifugal forces cause about 98% of the overall stress, whereas the forces and stresses caused by temperature and pressure differences have almost no influence. With regard to manufacturing aspects several materials are worth considering. But as the centrifugal force correlates directly with the density of the impeller material, lightweight materials are necessary. Thus for the impeller design only specific materials were considered: high-strength aluminum, titanium and carbon fiber appeared to be adequate choices. In order to reduce the mechanical stress the modification of the following parameters appeared to be the most relevant: rotational speed, blade thickness in means of mass reduction, the shroud radiuses and the blade geometry in terms of wrap angle, high twists and rakes in combination with the grade of tangential displacement in radial direction.

3.4 Basic Compressor Design

In order to fulfill the requirements for structural stability, minimizing the compressor size can be identified as major goal of the rotor design. So the outlet diameter should not exceed a certain given size. Otherwise the centrifugal force F_{fc} and stress σ_{max} induced by the increasing impeller tip speed u_2 would exceed the tolerable limit. One important parameter for a small outlet diameter is a high flow coefficient φ, according to equation 1.

$$D_2 = \sqrt{\frac{V_1}{\pi 4\, u_2 \varphi}} \quad (1)$$

A higher flow coefficient is reached when the specific volume is decreased. But at the same time a higher flow coefficient results in a larger axial compressor length, which induces an increasing bearing span.

$$\frac{p_2}{p_1} = \left[\frac{\Delta h_{tot}}{u_2^2}\,(\kappa - 1) M_{u2}^2 + 1\right]^{\frac{\kappa \eta_p}{\kappa - 1}} \quad (2)$$

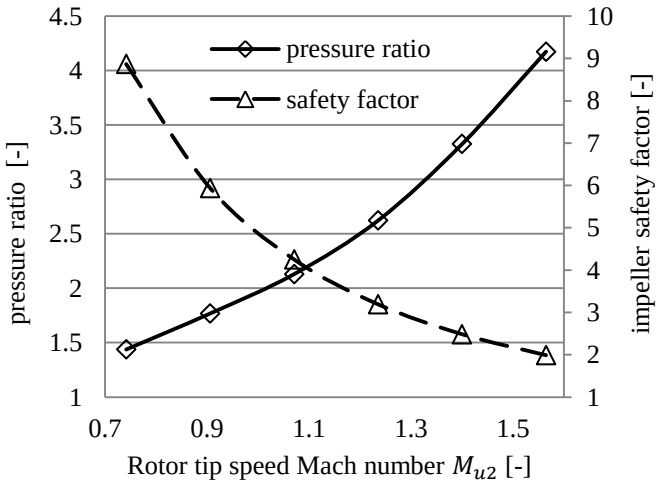

Figure 3: Pressure ratio and impeller safety factor over the tip speed Mach number

In figure 3 the relation between compressor pressure ratio, tip speed Mach number M_{u2} and impeller safety factor for the designed impeller of optimization step 4 is shown. The pressure ratio strongly depends on the tip speed Mach number (equation 2) and the isentropic exponent κ. Also in this diagram the influence of the safety factor is shown for the case of high strength aluminum with a maximum tensile strength (TS) of up to 550 MPa and is calculated according to equation 3. The safety factor of the impeller characterizes the ratio of maximum stress to allowable stress. It is a significant criterion to reach a high durability.

$$s_f = \frac{\sigma_{TS}}{\sigma_{max}} \quad (3)$$

The main goal is to reduce the high Mach number. A high Mach number leads to a narrower operating envelop of the compressor with a surge and choke point near the design point. A compressor with lower M_{u2} has a wider operating range near surge and choke line and has a better efficiency because of lower gas dynamic losses.

4. MEANLINE ANALYSIS AND OPTIMIZATION OF THE ROTOR DESIGN

4.1 Meanline Analysis

The design study for the turbo compressor had been oriented towards the following targets: meet the requirements of the hybrid heat pump, increase the isentropic efficiency, reduce the mechanical stress, increase the volume flow and increase the operating range. The preliminary design of a radial impeller has been calculated by empirical correlations (Pfleiderer, 2005). These empirical correlations had been validated by analysis of performance data of real impellers. As a first step the impeller design from CFturbo has been integrated in ANSYS Vista CCD and then exported into ANSYS DesignModeller. The flow optimization process was done based on the basic impeller dimensioning according to figure 4 (a).

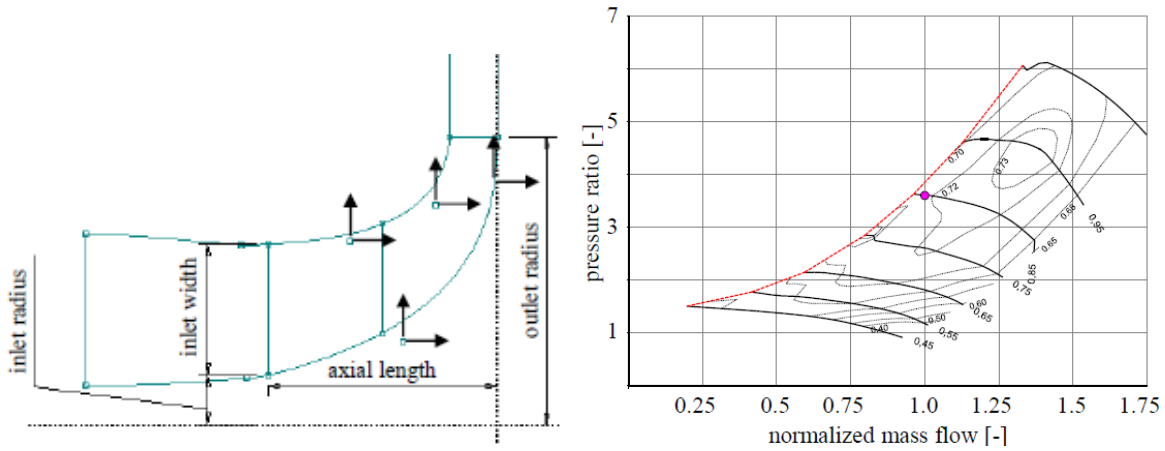

(a) (b)

Figure 4: Impeller Meanline Analysis (a) and radial compressor reference design without paying attention to the occurring stresses (b)

In order to allow a more qualified evaluation of the upcoming optimization results, an optimization in terms of fluid dynamic efficiency without regarding the stresses has been performed. The resulting operational map is shown in figure 4 (b).

The compressor design is limited by stress, vibration and material properties. It is a multi-objective design problem. Vibration induced by fluid dynamic interaction with stator and rotor is not investigated. The focus of this study is the improvement of the fluid dynamic performance, while stress is kept below tensile strength and deformation is minimized. The whole design procedure has been carried out iteratively, with identification of the optimal configuration by systematic variation of the governing design parameters, as described in the following section.

4.2 Coupled Fluid Dynamic and Structural Mechanic Optimization

The optimization is performed by the use of the software optiSLang 4.2.2 and pursued in four steps. The main difference to the meanline analysis is the consideration of stresses, resulting in two-dimensional (2D) optimizations. To get a better basis of assessment a one-dimensional (1D) optimization neglecting the stresses has been carried out

in advance, which was expected to bring the best possible results in means of specific compressor work, as described in the previous section (see figure 4 (b)). This design will further be referred to as ”reference design”. Prerequisite to a parametrical optimization is the parametrization of the model, with the side condition that a lower amount of varied parameters allows a better Coefficient of Prognosis (CoP) for the optimization results. Thus the impeller design created by Vista-CCD had to be parameterized and simplified. This way the impeller could be described by only 25 instead of the original 72 parameters.

1) On these 25 parameters a sensitivity analysis is performed in order to rank their influence on the output values. Based on the results of the sensitivity analysis then a 2D-optimization is performed, letting the objectives pressure ratio and efficiency perform against each other. For verification a compressor map, or compressor characteristic diagram (ChD), is being generated.

2) Additionally the four most influencing parameters are investigated with regard to pressure ratio, isentropic efficiency, choke and surge line. The results are described regarding the pressure ratio and operating range in the next section.

3) The influences of the geometry modifications are applied to the impeller design in order to match the desired operational limits as characterized by the target ChD. Now the design point should lie in the desired position. On the newly chosen design point a 1D-optimization is performed by means of meridional contour and rotational speed to gain a higher efficiency. In this case only a 1D-optimization is necessary as the parameters with the largest influence on the stresses rotational speed and outlet radius are restrained from growing during the optimization. Again a verification by use of an ChD analysis is performed.

4) In the next step the number of blades and their shape has been optimized in a 2D-optimization based on a further sensitivity analysis. Key figures for the optimization are fluid dynamic efficiency and material stress which commonly react contrariwise on the change of the rotor design. Therefore, the best design is deduced by use of a Pareto-diagram. For verification purposes again a ChD is calculated.

5) Following a detailed investigation on undesired behavior has been performed. Based on this knowledge gain an innovative shape for the leading edge has been developed and integrated by use of a final optimization.

6) In the final step, step 2 has been repeated for the final design. The results are shown in the next section as well.

4.2.1 Overall Optimization (step 1): As a result of the multidimensional optimization in step 1, an isentropic efficiency of 51% at the design point has been achieved. It could also be observed that the design point, originally meant to lie at a pressure ratio of 3 at 85,000 RPM, was unintentionally moved up to a pressure ratio of 3.3. For part load operation with lower speed of rotation the characteristic diagram exhibits slightly higher efficiencies up 55 %. The operation with optimum efficiency is found close to the choke line, whereas a steep decrease of efficiency is found for operation with high flow rate close to the surge line.

4.2.2 Dominating Geometric Parameters (step 2 & 6): In step 2 and 6 of the optimization process, the four most influencing parameters, impeller axial length, outlet diameter or outlet radius as well as twist and rake of the blade leading and trailing edges are investigated with regard to the position of choke and surge line. The results of the parameter variations are presented in the following bullet points. For the first parameter variation a design mass flow of 4.0 g/s was chosen at the design speed of 85,000 RPM. The second variation was based on 6.0 g/s and 65,000 RPM

AXIAL LENGTH A shortening of the axial length results in a shift of the characteristic curve towards lower flow rates combined with a slight decrease of the pressure ratio, as shown in figure 5. An enlargement of the axial length results in a shift of the characteristic curve towards higher flow rates with a roughly constant pressure ratio. The behavior appears to be the same for both designs.

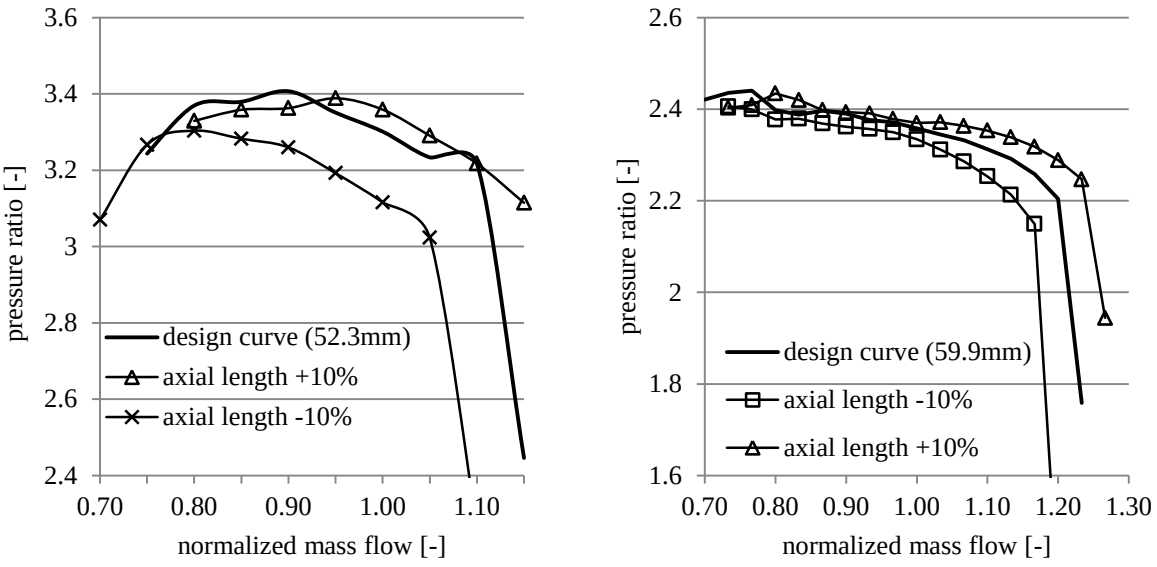

(a) (b)

Figure 5: Influence of the impeller axial length for the first (a) and final (b) design on the compressor design curve

OUTLET RADIUS An increase of the outlet radius – while reducing the outlet height in order to keep the outflow area constant – results in slightly higher flow rates and vice versa, accompanied by a strong influence on the pressure ratio. The effect displayed the same effect for both impeller designs (see figure 6).

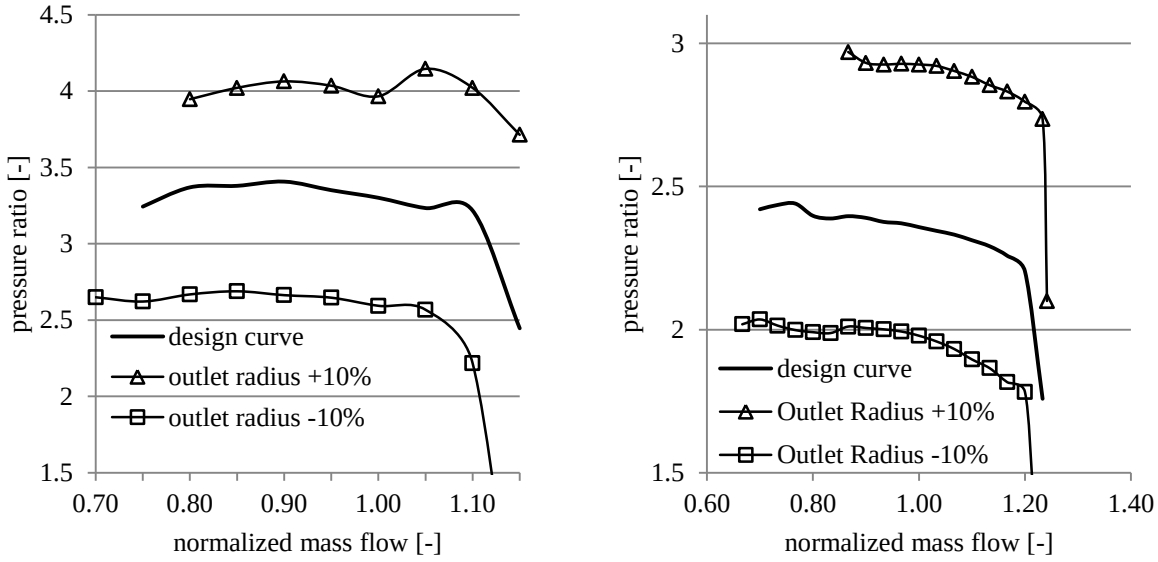

(a) (b)

Figure 6: Influence of the impeller outlet radius on the compressor design curves

TWIST The radial displacement in direction of rotation of the shroud tip at the leading edge compared to the hub tip is called twist. For the first design a positive change of the twist moves the characteristic curve towards lower flow rates and causes a slight increase of the pressure ratio. A negative change of the twist has the opposite effect (figure 7). For the final design the variation of the twist did not show significant results: The cause for this is estimated to lie in the new shape of the leading edge (compare figure 9).

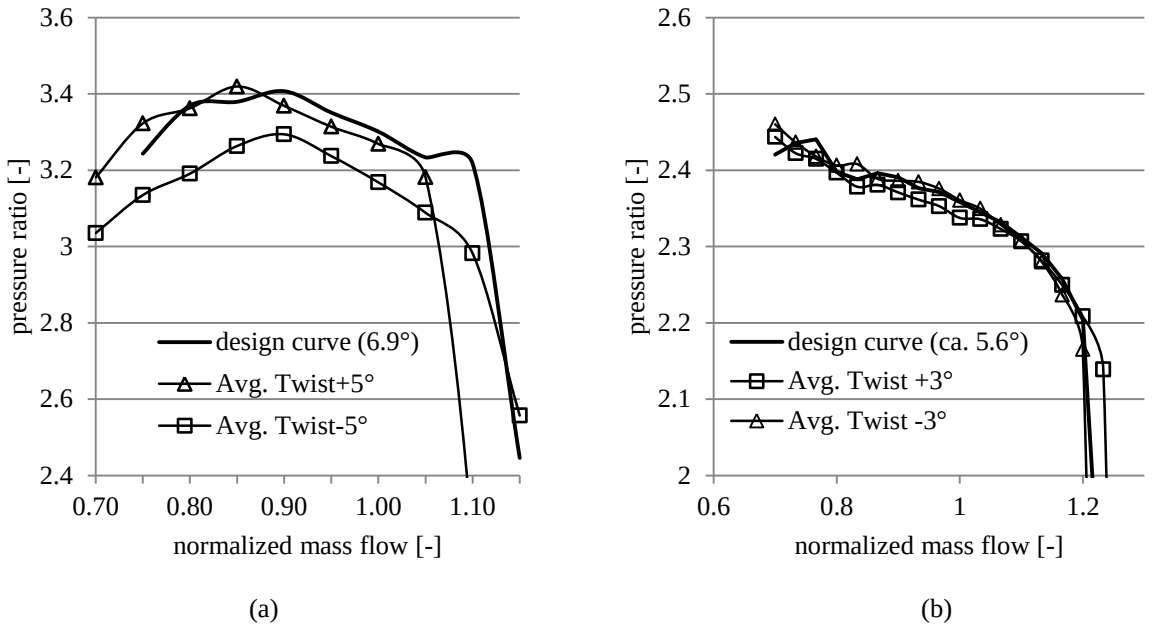

Figure 7: Influence of the variated twist on the first (a) and the final (b) design.

RAKE The radial displacement in direction of rotation of the shroud tip at the trailing edge of the compressor compared to the hub tip is called rake. For the first design a negative variation of the rake shifts the characteristic curves towards lower flow rates and lowers the pressure ratio. A positive change of the rake seems to have the same effects in a less pronounced manner (figure 8). The reason therefore lies in the previously performed optimization towards a higher pressure ratio. The design curve is already the one causing the highest pressure ratio, so that any modification worsens the result. For the final design, which hadn't been optimized for a maximal pressure raise, it can be seen as well that a lower rake appears to show better behavior in terms of pressure ratio.

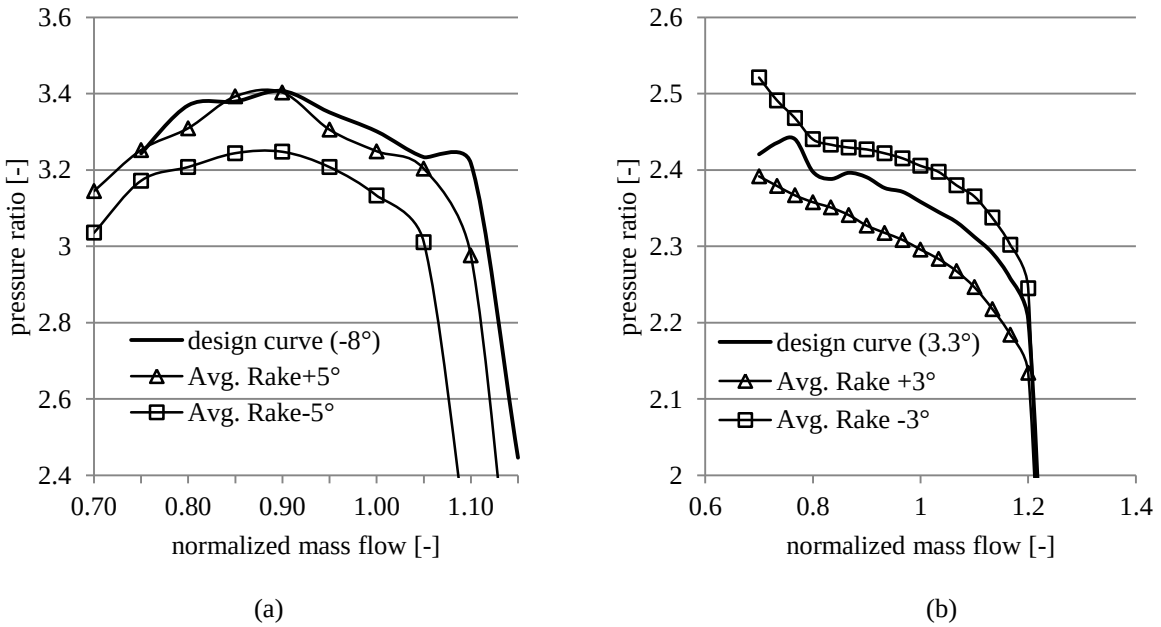

Figure 8: Influence of the rake variation onto the first (a) and final (b) design on the characteristic curve.

4.2.3 Step 5 and final Results: In step 5 the improved design from step 3 and 4 was analyzed in detail. Renderings of the simulations, both steady state and transient, showed a bad flow distribution within the passage. By

interdisciplinary applying methods from aerospace design methods the shape of the leading edge was customized and optimized for the given operating conditions. Figure 9 displays both the final design and the according characteristic diagram.

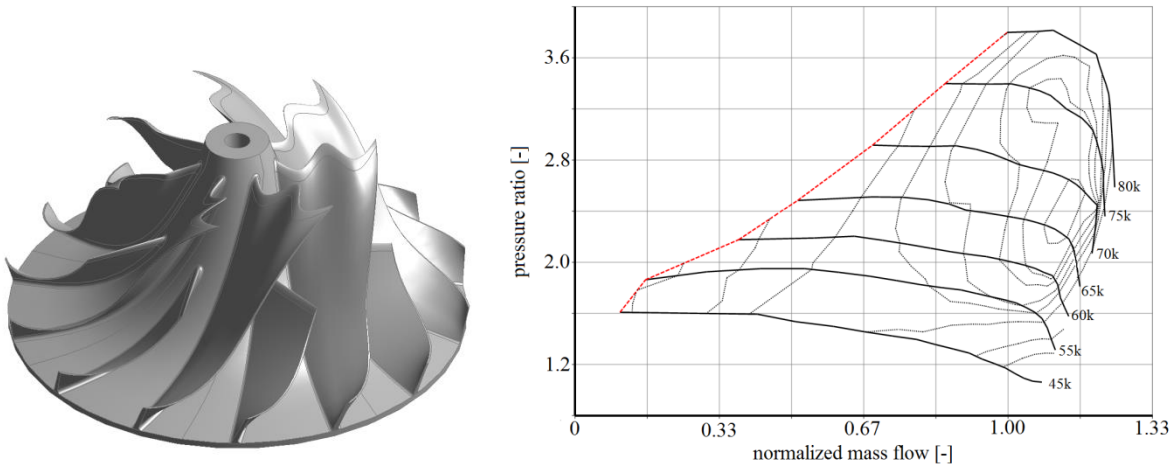

(a) (b)

Figure 9: Shape (a) and characteristic diagram (b) of the final design

5. CONCLUSION AND OUTLOOK

By systematic optimization of the compressor design an effective improvement in operating range and isentropic efficiency has been achieved, developing from the first to the resulting final Characteristic Diagram (ChD). The presented parameter variation showed the expected behavior for the variation of axial length and outlet radius as standard turbomachinery parameters. For the other varied parameters it is interesting to see how the potential for further increase in pressure ratio moved from the leading edge to the trailing edge.

As next step of the development process the thickness distribution along the rotor contour will be optimized for reduction of stress and distortion with regard to mechanical stability. The following steps are the validation of the calculated compressor in the compressor test rig at Munich University of Applied Sciences and the integration of the compressor into the absorption cycle for demonstration of the hybrid concept..

NOMENCLATURE

σ	Von-Mises stress	(MPa)
D_2	Impeller outlet diameter	(m)
c	Speed of Sound	(m/s)
h	Enthalpy	(J/kg)
M_u	Peripheral Mach Number	(-)
RPM	Speed of Rotation	(rev/min)
p	Pressure	(Pa)
T	Temperature	(C, K)
F_{cf}	Centrifugal force	(N)
u_2	Impeller peripheral speed	(m/s)
$\dot{V}_1$	Volumetric flow rate compressor inlet	(m^3/s)
$\dot{m}$	Massflow	(kg/s)
η	Isentropic compressor efficiency	(-)
κ	Conditional isentropic coefficient	(-)
γ	molecular mass	(kg/mol)
Π	Pressure ratio	(-)
s_f	Safety factor	(-)
φ	Flow rate coefficient	(-)

ChD	Characteristic Compressor Diagram
EH	Electrical Heat Coefficient
TS	Tensile Strength
EM	Electric Machine
CoP	Coefficient of Prognosis
CHP	Combined Heat and Power Unit
RANS	Reynolds-averages Navier-Stokes

REFERENCES

Alefeld, G. and Ziegler, F. (1985). Advanced heat pump and airconditioning cycles for the working pair H2O/ LiBr: domestic and commercial applications. *ASHRAE Transaction,* Honolulu

Eckert, T., Helm, M., Grassel, A., and Schweigler, C. (2015) Lithium Bromide/ R718 Hybrid sorption & compression cycle. *International Congress of Refrigeration*, Yokohama

Eckert, T., Dostal, L., Helm, M., Schweigler, C. (2016), Design of a Centrifugal Turbo Compressor with the Working Fluid Water for the Operation in a Hybrid Sorption / Compression Heat Pump Cycle, *ASME Turbo Expo 2016*, Seoul

Helm, M., Eckert, T., and Schweigler, C. (2015). Hybrid Water/ LiBr Absorption Chiller Boosted by High-Speed Turbo Compressor. *6th Int. Conf. Solar-Air-Conditioning,* Rome

Koren, A. and Ophir, A. (1996). Water vapor technology. *Proc. IIR Conf. Applications for Natural Refrigerants*, Aarhus

Madsboell, H. and Minds, G. (1995). A 2 MW Industrial Chiller using Water as Refrigerant. *Proc. IIR Conf. Applications for Natural Refrigerants*, Aarhus

Madsboell, H. (2011) Development of new type of compact, high efficient and cost effective axial compressor for commercial chillers with water as refrigerant. *International Congress of Refrigeration,* Prague

Madsboell, H., Weel, M. and Kolstrup, A. (2015). Development f a water vapor compressor for high temperature heat pump applications. *International Congress of Refrigeration*, Yokohama.

Mueller, N. and Kharazi,A. (2006). Comparing water (R718) to other refrigerants. *ASME Int. Mechanical Engineering Congress and Exposition, IMECE2006-13341*, Chicago

Niebergall, W. (2011). *Sorptions-Kältemaschinen.* Springer, 7th edition.

Paul, J. (2007). State of the art for cooling with water as refrigerant (R718). *Proc. IIR Conf. of Refrigeration,* Bejing

Pfleiderer, C. and Petermann, H. (2005). *Strömungsmaschinen. Klassiker der Technik*. Springer, 7th edition, Berlin.

Sarevski, M.N. and Sarevski, V.N. (2012). Preliminary Study of a Novel Compact R718 Water Chiller with Integration of a Single Stage Centrifugal Compressor and Two-Phase Ejectors. *Int. J. of Refrigeration*

Schweigler C. (1999). *Kälte aus Fernwärme: Konzept, Auslegung und Betrieb der Single-Effect/ Double-Lift-Absorptionskälteanlage: Doktorarbeit*. Technische Universität München, München.

Ziegler, F. (1991). Kompressions-Absorptions-Wärmepumpen, *Volume Nr. 34 of Forschungsberichte des Deutschen Kälte-und Klimatechnischen Vereins DKV,* Stuttgart

Ziegler, F., Kahn, Summerer, F., Alefeld, G. (1993). Multi-effect absorption chillers. *Int. J. of Refrigeration, volume 16.*

Ziegler, F. (2009) Sorption heat pumping technologies: Comparisons and challenges. *Int. J. of Refrigeration, volume 32*.

ACKNOWLEDGEMENT

This project is funded by the German ministry of Education and Research within the program ”Forschung an Fachhochschulen” with the grant number 03FH023I3.